Experimental Neurology 314 (2019) 46–57

Contents lists available at ScienceDirect

Experimental Neurology

journal homepage: www.elsevier.com/locate/yexnr

Research paper

Astrocytes migrate from human neural stem cell grafts and functionally integrate into the injured rat spinal cord

Brian V. Lien[a], Mark H. Tuszynski[b,c,*], Paul Lu[b,c,*]

[a] Division of Biological Sciences, University of California - San Diego, La Jolla, CA, USA
[b] Department of Neurosciences, University of California - San Diego, La Jolla, CA, USA
[c] VA San Diego Healthcare System, San Diego, CA, USA

ARTICLE INFO

Keywords:
Astrocytes
Astroglia
Migration
Spinal cord injury
Blood-spinal cord barrier
Neurotransmitter regulation
Glial scar

ABSTRACT

Neural stem cells (NSCs) can differentiate into both neurons and glia after transplantation into spinal cord injury (SCI) sites. The neuronal component of stem cell grafts has the potential to form functional synaptic relays across the lesion site. The glial component may reform a blood-spinal cord barrier, support neuronal function, and contribute to remyelination. We performed a long-term, 1.5-year time course study focused on astrocyte migration, differentiation, integration, and safety following human NSC transplantation into C5 hemisection sites in immunodeficient rats. NSCs that adopted a neuronal fate did not migrate from the lesion site. In contrast, transplanted cells that adopted astrocyte fates exhibited long distance migration from the lesion site through host white matter in rostrocaudal directions. These cells migrated slowly at a mean rate of 2–3 mm/month, divided as they migrated, and gradually differentiated into astrocytes. After 1.5 years, human astrocytes migrated nine spinal cord segments, caudally to the mid-thoracic level, and rostrally into the brainstem. The migrated human astrocytes joined the endogenous population of astrocytes in the host spinal cord, extended perivascular endfeet towards host pericytes and endothelium, formed interspecies and intraspecies perivascular astrocytic networks connected by gap junctions, and expressed glutamate transporter proteins in perisynaptic processes, suggesting structural and functional integration. No adverse consequences of this extended glial migration were detected. Adjacent to the lesion site, chronic host astrocytic upregulation was significantly attenuated by NSC grafts. Thus, human astrocytes can migrate long distances from sites of SCI and safely integrate into the host central nervous system.

Significance statement: Neural stem cell (NSC) grafts are a candidate therapy for spinal cord injury (SCI). Here we report an 18-month study of astrocyte survival and migration from sites of SCI in immunodeficient rats. NSC grafts significantly attenuate host astrocyte reactivity at the lesion/host interface. Intra-graft astrocytes integrate into the host blood-spinal cord barrier (BSCB) and widely express glutamate transporter proteins characteristic of neurotransmitter regulation. Notably, astrocytic components of NSC grafts exhibit gradual yet extensive migration after implantation into the mid-cervical injury site; neurons do not migrate at all. This extensive astrocyte migration is not detectably associated with adverse outcomes anatomically or behaviorally.

1. Introduction

When grafted into sites of spinal cord injury (SCI), neural stem cells (NSCs) differentiate into both neurons and glia, including oligodendrocytes and astrocytes (Lu et al., 2012; Lu et al., 2014; Kadoya et al., 2016; Lu et al., 2017; Rosenzweig et al., 2018). The neuronal component of stem cell grafts enables formation of neuronal relays across sites of spinal cord injury (SCI) and can support partial functional motor recovery (Lu et al., 2012; Kadoya et al., 2016; Lu et al., 2017; Rosenzweig et al., 2018). The glial component of stem cell grafts, especially the oligodendrocyte component, may myelinate graft- and host-derived neurons (Keirstead et al., 2005; Karimi-Abdolrezaee et al., 2006; Hawryluk et al., 2014; Salewski et al., 2015).

To date, the astrocyte component of glia derived from NSC grafts after SCI has not been studied extensively. During central nervous system (CNS) development, gliogenesis follows neurogenesis (Semple et al., 2013; Gallo and Deneen, 2014). One key feature of astrocyte development involves the migration of astrocyte precursors away from the germinal centers prior to differentiation (Gallo and Deneen, 2014). During migration, immature glia, including astrocyte precursors,

* Corresponding author: Dept. Neurosciences, 0626 University of California, San Diego, La Jolla, CA 92093, USA.
E-mail addresses: mtuszynski@ucsd.edu (M.H. Tuszynski), plu@ucsd.edu (P. Lu).

https://doi.org/10.1016/j.expneurol.2019.01.006
Received 14 October 2018; Received in revised form 13 December 2018; Accepted 12 January 2019
Available online 15 January 2019
0014-4886/

proliferate to increase their numbers before, during, and after migration (Canoll and Goldman, 2008; Klambt, 2009; Tien et al., 2012; Schitine et al., 2015). Interestingly, the peak of gliogenesis coincides with blood vessel growth, dendrite elaboration, and synapse establishment, wherein astrocytes form crucial interactions with vasculature and neurons (Barres, 2008; Semple et al., 2013). Astrocytes help form and maintain the blood-brain barrier (BBB); they also support neuronal function by secreting neurotrophic factors, recycling neurotransmitters, maintaining CNS homeostasis, and regulating synaptic plasticity (Abbott et al., 2006; Barres, 2008; Haas and Fischer, 2013). Beyond normal development, the migration of astrocytes has been demonstrated by transplantation of NSCs and glial progenitors, mostly in the developing embryonic (Brustle et al., 1998) or postnatal (Han et al., 2013; Windrem et al., 2014) CNS. The migration of astrocytes has also been demonstrated in the adult CNS after transplantation of neural precursor cells or glial progenitors (Han et al., 2004; Lepore et al., 2004; Jin et al., 2011; Haas and Fischer, 2013; Chen et al., 2015). These studies did not, however, characterize the differentiation, migration, and integration of astrocytes after transplantation of human NSCs into the injured spinal cord. Indeed, the injured CNS environment differs from that of the developing or intact CNS and may thereby alter NSC differentiation, migration, and integration. For example, CNS injury elicits reactive astrogliosis that protects the CNS from further damage (Gallo and Deneen, 2014; Sofroniew and Vinters, 2010; Silver and Miller, 2004) and may influence the ability of CNS axons to regenerate (Silver and Miller, 2004; Anderson et al., 2016).

In this study, we sought to examine the extent to which astrocyte differentiation contributed to NSC graft function after SCI, and how graft-derived astrocyte migration from the lesion site influences host systems. We previously reported that human NSCs grafted into injured immunodeficient rats exhibit a prolonged period of neuronal and glial maturation in sites of injury (Lu et al., 2017). Using material from that study, the present study examined in detail the maturation, integration and migration of astrocytic components of human NSC grafts. We find that grafts attenuate host astrocytic reactivity at host/lesion interfaces, and that astrocyte derivatives within grafts form a blood-spinal cord barrier and express glutamate transporters; furthermore, astrocytes exhibit gradual and extensive migration out from grafts, without apparent deleterious effects on the host.

2. Materials and methods

In this time-course study, 26 immunodeficient rats received a C5 lateral hemisection followed by transplantation of H9 human embryonic stem cell (ESC)-derived NSCs (H9-NSCs) 2 weeks after injury. Previously, we published data from this study describing the neuronal component of NSC grafts and late recovery of motor function, while only briefly describing the glial component of NSC grafts (Lu et al., 2017). Here, we report a comprehensive analysis of the migration, differentiation, and integration of graft-derived glia over a period of 1.5 years. Further details regarding the procedures involved in this study are described below.

2.1. Lesion and transplantation surgeries

Animal experiments were approved by the Institutional Animal Care and Use Committee (IACUC) of the Veterans Administration (VA) San Diego Healthcare System. National Institutes of Health (NIH) guidelines for laboratory animal care and safety were strictly followed. For this study, 26 adult female athymic T-cell immunodeficient rats were obtained from the Harlan Laboratories (Lu et al., 2017). For our lesion model, we used the C5 lateral hemisection (Lu et al., 2012; Lu et al., 2017). Animals were anesthetized using a mixture of ketamine (25 mg/ml), xylazine (1.3 mg/ml), and acepromazine (0.25 mg/ml) under sterile conditions. At the C5 segment, a dorsal laminectomy was performed, the dura was incised, and a C5 right lateral hemisection was performed using iridectomy scissors and microaspiration, removing a 2-mm-long block of the right hemicord. The lesion was visually verified to ensure complete transection. Postoperative treatment included daily subcutaneous banamine (2.5–5 mg/kg) and ampicillin injections (3–5 mg/kg) for 1–2 weeks.

Human H9 ESC-derived NSCs were purchased from Invitrogen (catalog N7800–100) (Thomson et al., 1998; Zhang et al., 2001) and cultured on a CELLstart coated flask (Thermo Fischer Scientific) as described previously (Lu et al., 2017). To visualize the survival, differentiation, migration, and process outgrowth of transplanted NSCs in vivo, we transduced these H9 NSCs with lentiviruses expressing green fluorescent protein (GFP) prior to transplantation, resulting in transduction of approximately 95% of NSCs. Cells were grafted in a fibrin matrix to retain cells in the lesion cavity, consisting of fibrinogen (F6755; Sigma; 25 mg/ml) and thrombin (T5772; Sigma; 25 U/ml). To support survival of the transplanted NSCs in vivo, the following growth factors were included in the growth factor cocktail: brain-derived neurotrophic factor (452–02; Peprotech; 50 μg/ml), neurotrophin-3 (450–03; Peprotech; 50 μg/ml), platelet-derived growth factor (P30736; Sigma; 10 μg/ml), insulin-like growth factor 1 (I8779; Sigma; 10 μg/ml), epidermal growth factor (E1257; Sigma; 10 μg/ml), basic fibroblast growth factor (F0291; Sigma; 10 μg/ml), acidic fibroblast growth factor (F5542; Sigma; 10 μg/ml), glial cell line-derived neurotrophic factor (G1401; Sigma; 10 μg/ml), hepatocyte growth factor (HGF; Sigma; 10 μg/ml), and calpain inhibitor (M6690; Sigma; 50 μM) (Lu et al., 2012). NSCs were harvested and mixed with the aforementioned fibrin matrix and growth factors at a concentration of 250,000 cells/μl. 4 μl of cells were injected into the lesion cavity 2 weeks after injury, a clinically relevant time-point for intervention.

Three animals died after the C5 hemisection, leaving twenty-three subjects. These 23 animals were randomly divided into one of two groups: one group received human NSC grafts (n = 18), and one group served as lesioned controls without grafts (n = 5). Animals in the experimental group were perfused either 1 month (n = 3), 3 months (n = 3), 6 months (n = 5), 12 months (n = 3) or 18 months (*n* = 4) after grafting. Animals in the control group received C5 hemisections and vehicle injections of the fibrin matrix containing the growth factor cocktail, but without NSCs. Animals in the control group were perfused 12 months after vehicle injection.

2.2. Histology

At varying time-points, animals were transcardially perfused with 4% paraformaldehyde in a 0.1 M solution of phosphate buffer at pH 7.4 and post-fixed overnight in the same solution at 4 °C. Brains and spinal cords were dissected out and suspended in 30% sucrose for three days. We removed a 12-mm portion of the spinal cord with the lesion/graft site at the center for horizontal sectioning, the entire right hemisphere of the brain for sagittal sectioning, and 1–2 mm segments of C2, C8, T6, T12, and L4 of the spinal cord for coronal sectioning. All sections were cut on a cryostat set at 30 μm thickness and sections were collected serially into 24-well plates.

2.3. Immunohistochemistry

Antigen blocking and tissue permeabilization of free floating brain and spinal cord sections were accomplished using 5% donkey serum and 0.25% Triton X-100 in Tris-Buffered Saline (TBS) for 1 h on a shaker at room temperature, followed by incubation of primary antibodies in the same solution overnight at 4 °C. Sections were rinsed in 3% donkey serum and 0.25% Triton X-100 in TBS. Alexa 488-, 594-, or 647-conjugated donkey secondary antibodies against the species of individual primary antibodies (Invitrogen, Thermo Fisher Scientific; 1:500) were incubated in the aforementioned solution for 2.5 h on a shaker at room temperature. Sections were then washed with TBS, mounted on uncoated slides, and coverslipped with Fluoromount-G

(SouthernBiotech). The following primary antibodies were used: (a) GFP rabbit polyclonal antibody (GFP-1020; Aves; 1:1000) was used to assess survival, differentiation, and migration of grafted human cells; (b) Human-specific nuclei (hNu) mouse monoclonal antibody (mab1281; Millipore; 1:500) was used to assess migration of grafted human cells; (c) Ki67 rabbit polyclonal antibody (gtx16667; Genetex; 1:500) was used to assess proliferation of migrated grafted human cells; (d) Human-specific vimentin mouse monoclonal antibody (nbp2–44,833; Novus Biologicals; 1:500) was used to assess differentiation of grafted human cells into glial progenitor cells; (e) Human-specific glial fibrillary acidic protein (hGFAP) rabbit polyclonal antibody (TA302094; Origene; 1:500) was used to assess differentiation and integration of human grafted-derived astrocytes; (f) glial fibrillary acidic protein (GFAP) goat polyclonal antibody (sc-6170; Santa Cruz Biotechnology; 1:500) was used to assess endogenous rat as well as human graft-derived populations of astrocytes; (g) adenomatous polyposis coli (APC) mouse monoclonal antibody (OP80; Oncogene; 1:500) and myelin basic protein (MBP) rabbit polyclonal antibody (AB980; EMD Milliopore; 1:500) were used to assess human graft-derived oligodendrocytes; (h) RECA1 mouse monoclonal antibody (ab9774; Abcam; 1:500) was used to assess whether graft-derived astrocytes interacted with host endothelial cells; (i) human-specific Nestin mouse monoclonal antibody (ab18102; Abcam; 1:500) was used to assess whether grafted neural stem cells migrated; (j) platelet-derived growth factor receptor β (PDGFRβ) rabbit polyclonal antibody (sc-432; Santa Cruz Biotechnology; 1:500) was used to assess whether human graft-derived astrocytes interacted with endogenous pericytes; (k) Connexin 43 (CX43) rabbit polyclonal antibody (48-3000; ThermoFisher Scientific; 1:200) was used to assess whether human graft-derived astrocytes formed perivascular astrocytic networks; (l) microtubule-associated protein 2 (MAP2) mouse monoclonal antibody (556320, BD Bioscience; 1:500) was used to assess whether human graft-derived astrocytes interacted with the somatodendritic domain of human grafted-derived neurons; (m) a glutamate transporter isoform (GLT1) guinea pig polyclonal antibody (AB1783; Millipore; 1:250) was used to assess whether human graft-derived astrocytes expressed glutamate transporter proteins in the lesion/graft site.

2.4. Quantification

To quantify the GFAP immunofluorescent intensity at the lesion/graft boundary, the hemisection site in two randomly selected sections per subject was imaged on an Olympus Fluoview FV1000 confocal microscope at 100× magnification at uniform exposure levels in both the control group sacrificed 1 year after vehicle injection and in the 12 month group sacrificed 1 year after NSC grafting. The GFAP labeling from a defined region of 0.5 mm width in the rostral direction from the lesion/graft boundary in each image was measured using ImageJ to determine the percentage of GFAP immunofluorescent intensity in the control group versus the 12 month group ± SEM.

Migrated human cells were defined as hNu+/GFP+ for quantification. All hNu+/GFP+ puncta were counted on images taken by a Keyence BZ-X710 all-in-one microscope and camera at 200× magnification to quantify the total number of migrated human cells in two randomly selected coronal C2 spinal cord sections per subject. The total number of hNu+/GFP+ puncta per section was then averaged with other subjects in the same group (6, 12, and 18 months after grafting) to determine the mean number of cells that migrated three spinal cord segments (6–9 mm) rostral to the lesion/graft site ± SEM.

Proliferating migrating human cells were defined as Ki67+/hNu+/GFP+ puncta for quantification. Ki67+/hNu+/GFP+ puncta and hNu+/GFP+ puncta were counted on images taken by an Olympus BX53 digital fluorescence microscope at measured distances 0–2 mm, 2–4 mm, and 4 mm + from the leading edge of hNu+/GFP+ human cell migration. Two sagittal sections per subject were quantified in the 18-month group in a randomly chosen field (fixed box size 1600 × 1200 pixels at 100× magnification) at each measured distance. The percentage of dividing human cells was calculated by dividing the number of Ki67+/hNu+/GFP+ colocalizing puncta by the total number of hNu+/GFP+ colocalizing puncta, then averaged at each measured distance to determine the mean percentage of dividing cells per section ± SEM.

Images of astrocytes from the left (non-grafted) lateral region and right (grafted) lateral region in two randomly selected C2 coronal spinal cord sections per subject was taken using an Olympus BX53 digital fluorescence microscope at uniform exposure levels for quantification. For quantification, subjects from the group sacrificed 18 months after NSC grafting were used. Human astrocytes were defined as GFAP+/DAPI+/hNu + while rat astrocytes were defined as GFAP+/DAPI+/hNu-. Randomly chosen fields (fixed box size 800 × 600 pixels at 200× magnification) in the left lateral region and right lateral region of each C2 section were quantified to compare the number of human and rat astrocytes in the non-grafted side versus the grafted side. The number of rat and human astrocytes counted in each section were averaged to determine the mean number of rat and human astrocytes in the non-grafted side or grafted side ± SEM.

2.5. Image acquisition

All images presented in figures were taken on either an Olympus Fluoview FV1000 confocal microscope or Keyence BZ-X710 all-in-one microscope and camera. Images presented in figures were enhanced uniformly for optimal contrast and brightness using Adobe Photoshop CS6. Images used to quantify GFAP immunofluorescence intensity on ImageJ were not modified.

2.6. Experimental design and statistical analysis

In all quantification procedures, observers were blind to the nature of the experimental manipulation. Comparisons among multiple groups were tested by ANOVA (JMP software) at a designated significance level of $P < .05$, followed by non-parametric test using the Wilcoxon method. Comparisons between two groups were tested by Student *t*-test (JMP software) at a designated significance level of $P < .05$. All data are presented as the mean ± SEM.

3. Results

3.1. Neural stem cell xenografts attenuated reactive astrogliosis

After CNS injury, nearby astrocytes undergo reactive astrogliosis, which is characterized by upregulation of GFAP, astrocyte hypertrophy, and astrocyte proliferation (Silver and Miller, 2004; Sofroniew and Vinters, 2010; Anderson et al., 2016). Previous studies have reported that reactive astrogliosis is attenuated after transplantation of immature astrocytes into the adult CNS (Smith et al., 1986). In the injured spinal cord, glial-restricted progenitor cells (Jin et al., 2011) and neural progenitor cells (Kadoya et al., 2016) also attenuate reactive astrogliosis; however, these observations were based on short-term studies where animals were sacrificed 8 weeks and 6 weeks after injury, respectively. We determined whether astrogliosis was attenuated 1 year after NSC grafting by immunolabeling for GFAP at the lesion boundary. In lesioned control animals, GFAP immunoreactivity was increased at the host/lesion interface as previously reported (Smith et al., 1986; Silver and Miller, 2004; Sofroniew and Vinters, 2010; Fawcett, 2009; Anderson et al., 2016) (Fig. 1A–B). In grafted animals, there was a significant attenuation of GFAP labeling at the host/lesion/graft interface one year after SCI (Fig. 1C–F). To quantify the intensity of GFAP at the lesion site, ImageJ was used to measure the percentage of the field occupied by GFAP immunoreactivity (Kadoya et al., 2016; Jones and Tuszynski, 2002). Quantification revealed that 76 ± 2.5% the 500 μm region adjoining the lesion site exhibited GFAP immunoreactivity in

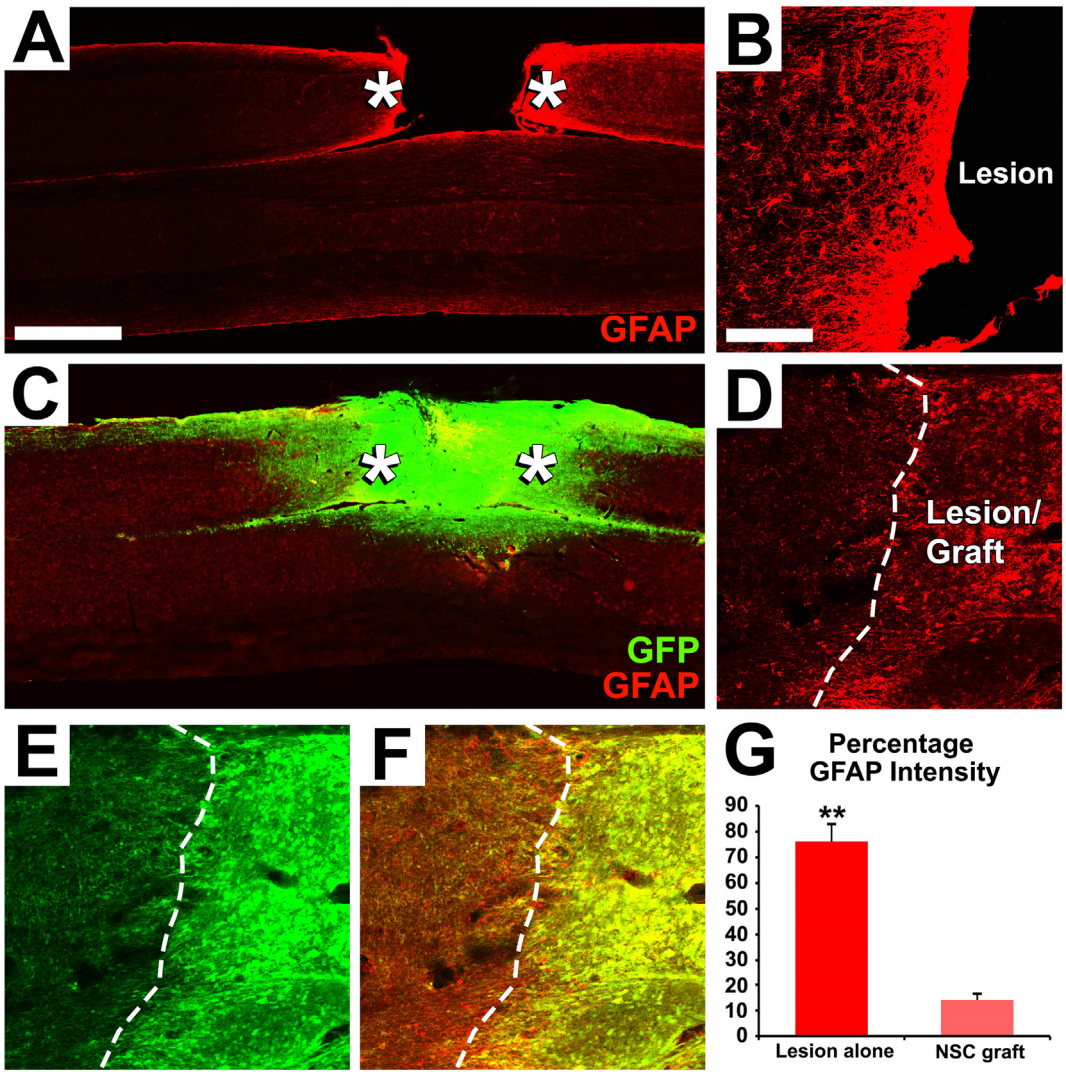

Fig. 1. Human NSC grafts attenuate reactive astrogliosis.
(A–F) Images were taken 12 months after vehicle or NSC grafting. Horizontal sections are shown in all panels with rostral left, caudal right. **(A) GFAP** immunoreactivity (red) at the lesion boundary in control animals that received vehicle injection without NSC grafts after hemisection. A region of **GFAP** upregulation (red) is present at the lesion boundary indicated by the asterisks; the rostral host/lesion boundary is shown at higher magnification in the panel B. **(B)** High magnification view of persistently upregulated GFAP immunoreactivity after 12 months in lesioned controls. **(C)** Twelve months after lesions and NSC grafts, **GFAP** immunoreactivity at the lesion boundary is reduced relative to lesioned controls. The lesion boundary indicated by the asterisk is magnified in the adjacent panels. **(D-F)** Dashed lines indicate the graft-host interface. **(D)** High magnification of the host/lesion/graft interface, demonstrating attenuation of **GFAP** immunoreactivity. (E) **GFP** + graft-derived cells at the host/graft interface. **(F)** In the merged image, **GFAP**+/**GFP**+ human astrocytes (yellow) are present within the graft. **(G)** Quantification of **GFAP** intensity at the host/lesion boundary. Mean ± SEM. $^{**}P < .01$, Student's *t*-test. Scale bar, 1 mm (A, C); 200 μm (B, D-F) (For interpretation of the references to colour in this figure legend, the reader is referred to the web version of this article.)

lesioned controls, compared to 14.1 ± 6.6% in grafted animals ($t = -8.8$, df = 3, $p = .006$ by Student's *t*-test; Fig. 1G).

3.2. Grafted human cells gradually migrated in rostrocaudal directions

We observed gradual and progressive migration of grafted GFP+ cell bodies from the lesion site over a period of 18 months. To confirm that cells were indeed migrating from the graft and were not merely axons extending from human graft-derived neurons, we used hNu antibody to specifically immunolabel human nuclei (Fig. 2A-B). 1 month after grafting, we saw few migrated cells; however, we did observe GFP + fine processes that were likely axons, given the absence of adjacent GFP-labeled cell bodies, extending 4 mm from the graft into host white matter (Fig. 2C). As early as 3 months after grafting, migrated hNu +/GFP+ cells were visualized 4 mm from the graft (Fig. 2D). The number of migrated hNu+/GFP+ cells increased over time, and a substantial number of cells migrated 4 mm from the graft at 12 and 18 month time points (Fig. 2E–G). By 18 months, hNu+/GFP+ cells migrated up to 30 mm. In the caudal direction, cells migrated to the mid-thoracic level at T6 (30 mm), and in the rostral direction, cells migrated up to the medulla (15 mm). These cells migrated at a rate of 2–3 mm per month.

We used the hNu antibody to specifically label human nuclei and visualize the spatial distribution of migrated cells in coronal spinal cord sections at C2, three segments rostral to the lesion site. Interestingly, we observed migrated human cells exclusively in the host white matter over the 18 month study (Fig. 3A, C, E), which is consistent with studies showing that astrocyte progenitors migrate along axonal tracts during mammalian neural development (Klambt, 2009). Indeed, previous studies involving glial restricted precursor (GRP) cell allografts into rats also reported preferential migration of graft-derived glia along white matter tracts (Han et al., 2004). We did not observe migrating graft

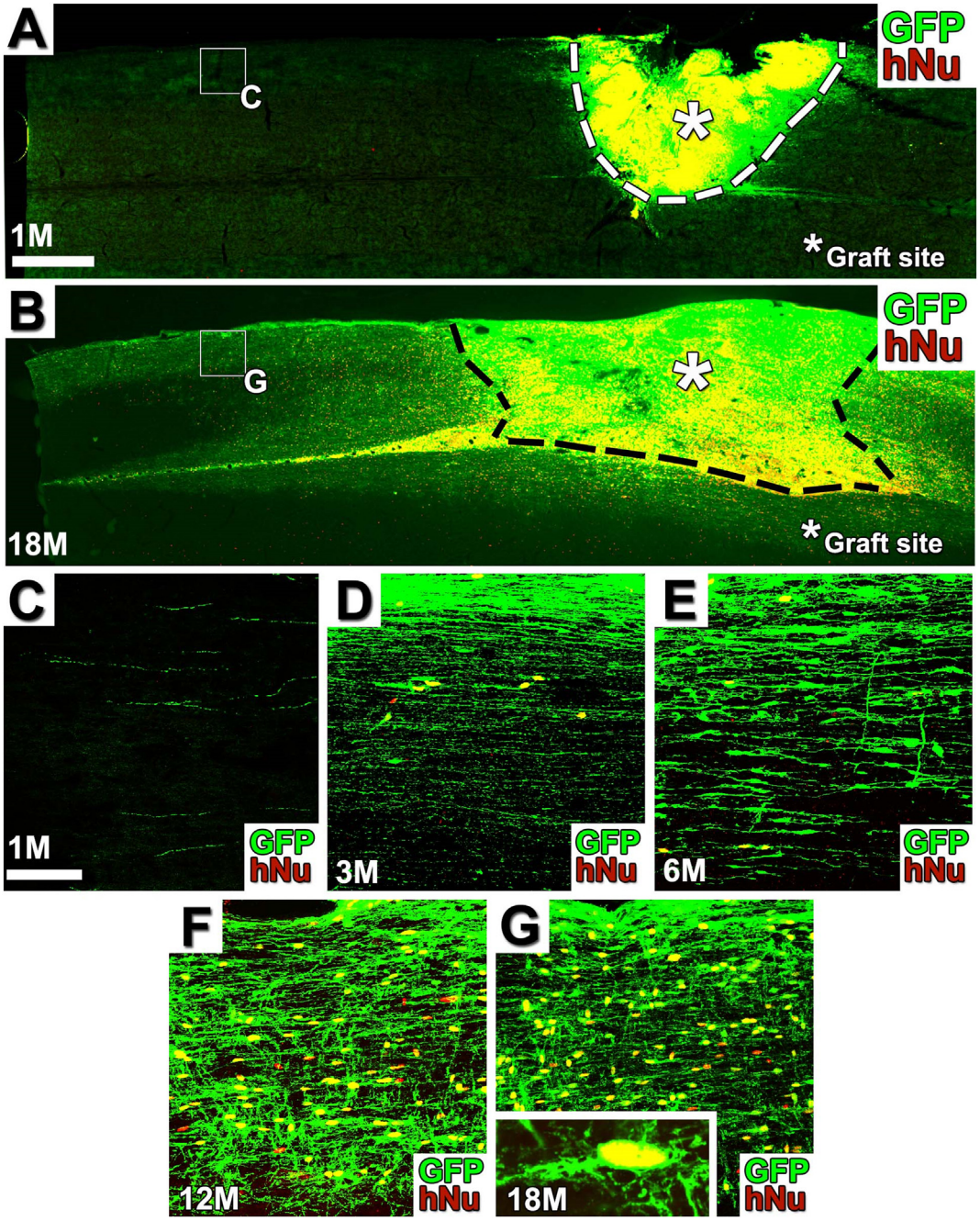

Fig. 2. Grafted stem cells gradually migrate from the lesion site from 1 to 18 months.
(A) Graft (asterisk) occupies the lesion cavity, 1 month post-grafting. Note that human NSCs remain within lesion site. Horizontal sections are shown in all panels with rostral left, caudal right. **(B)** 18 months after grafting, numerous GFP-labeled cells have migrated from the lesion site (shown at higher magnification in panel G); host/graft border is indicated by dashed line. Migration occurs through host white matter only, in both rostral (shown) and caudal directions. **(C)** One month after grafting, hNu/GFP labeled cells are not visible in host white matter at a point 4 mm rostral to the graft/lesion site except GFP+ fine processes identified as axons in our previous study (Lu et al., 2017). hNu labels human nuclei. **(D-G)** hNu+/GFP+ cells progressively increase in number at a point 4 mm rostral to the host/graft border by 3 mo (D), 6 mo (E), 12 mo (F) and 18 mo (G) after grafting (quantified in Fig. 3). Inset in panel G showing a migrated cell body and processes. Scale bar, 1 mm (A-B); 60 μm (C-G).

cells in host gray matter outside the lesion site (Fig. 3). After 6 months, few hNu+/GFP+ cells had migrated as far as C2 (Fig. 3A-B). However, by 12 and 18 months after grafting, many cells grafted into the C5 lesion site had migrated to the C2 level. Most migrated cells were present ipsilateral to the lesion, while some migrated cells moved into contralateral side (Fig. 3C-F). We quantified the total number of hNu+/GFP+ cells in coronal sections at C2 in subjects sacrificed 6 months, 12 months, or 18 months after grafting (Fig. 3G). The mean number of hNu+/GFP+ cells detected three segments rostral to the lesion/graft site increased proportionately over time ($Z = -2.0$, $p = .05$ by ANOVA and Wilcoxon test, comparing 6 months to 12 months; $Z = -2.2$, $p = .03$ by ANOVA and Wilcoxon test, comparing 6 months to 18 months).

3.3. Migrating grafted cells divide at the leading edge of migration

Because glia are known to divide as they migrate during neural development (Canoll and Goldman, 2008; Klambt, 2009; Tien et al.,

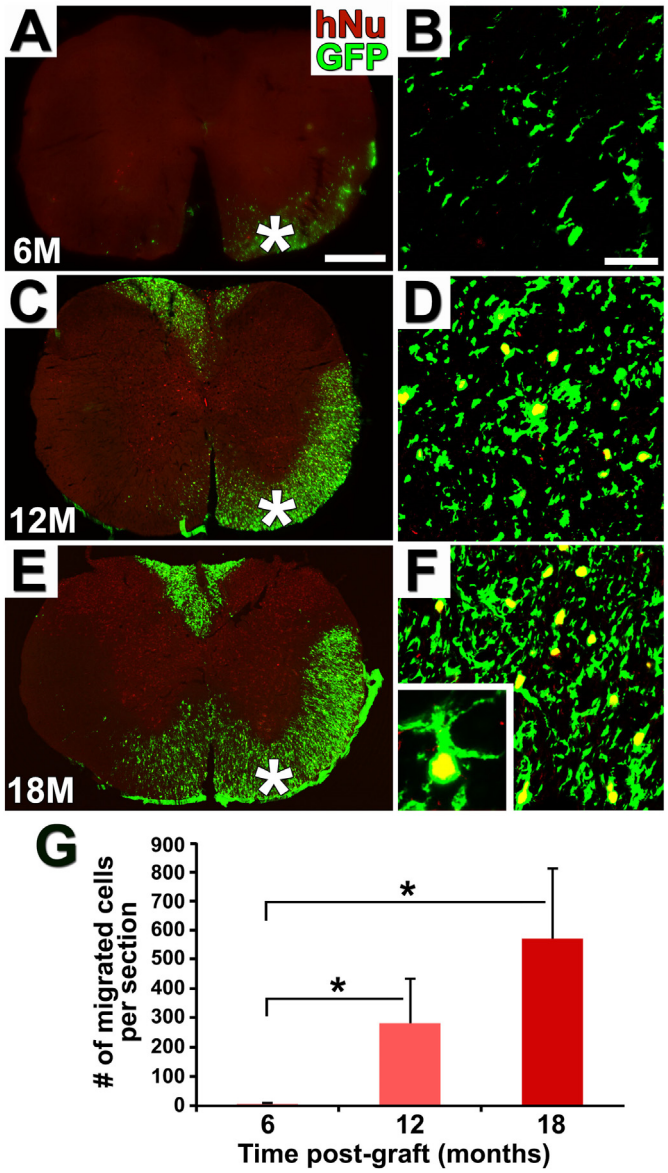

Fig. 3. Increased numbers of migrating cells over time, three spinal cord segments rostral to graft site.
(A, C, E) Spatial distribution of hNu + /GFP + nuclei in C2 coronal spinal cord sections among subjects sacrificed 6, 12, and 18 months after grafting. Asterisks represent area magnified in adjacent panels. Images were taken 3 spinal cord segments rostral to the graft/lesion site. There is a gradual increase in number of cells that migrated to C2 over time. **(B, D, F)** Higher magnification images of coronal C2 sections in subjects 6, 12, and 18 months after grafting. **(B)** GFP + axons or migrated cell processes, but very few nuclei, are visible 6 months after grafting. **(D, F)** hNu + /GFP + cells can be detected 12 months after grafting, and increase in number by 18 months. Inset in panel F showing a migrated cell body and processes. **(G)** Quantification of hNu + /GFP + cells per coronal C2 section. The number of migrated nuclei increased significantly over 18 months. *$P < .05$, ANOVA and Wilcoxon test compared to 6 mo. ± SEM. Scale bar, 400 μm (A, C, E); 30 μm (B, D, F).

2012), we used the cell proliferation marker, Ki67, to assess whether human cells grafted into the injured rat spinal cord divided as they migrated, defined as Ki67 + /hNu + /GFP + . The majority of Ki67 + /hNu + /GFP + cells were found within 2 mm of the leading edge of migration at the 6, 12, and 18 month time points (Fig. 4A–I). We quantified the number of Ki67 + /hNu + /GFP + cells and the total number of hNu + /GFP + cells in subjects sacrificed 18 months after grafting and found an average of 1.94 ± 0.17% dividing cells within a distance of 0–2 mm from the leading edge of cell migration, compared to only 0.04 ± 0.04% dividing cells within a distance of 2–4 mm from the leading edge, and no dividing cells at a distance > 4 mm from the leading edge ($Z = -2.2$, $p = .03$ by ANOVA and Wilcoxon test comparing 0–2 mm to 2–4; $Z = -2.3$, $p = .02$ by Wilcoxon test comparing 0–2 mm to > 4 mm) (Fig. 4J). In the majority of subjects in the 18-month group, the leading edge of rostral migration was found in the brainstem.

3.4. Migrating grafted cells differentiated into glial progenitors and astrocytes

To characterize the cell types migrating from the graft, we performed immunodetection experiments for a variety of neural cell types. We previously reported that NSCs that adopt a neuronal fate do not migrate (Lu et al., 2017). We endeavored to more fully characterize the cells migrating from the graft by using a human-specific vimentin antibody to specifically label graft-derived glial progenitor cells and a human-specific GFAP (hGFAP) antibody to label graft-derived astrocytes in coronal C2 sections. Three segments rostral to the lesion site, Vim + /GFP + and hGFAP + /GFP + immunoreactivity was detected by 12 and 18 months but not 6 months after grafting (Fig. 5A-B). We also used the human-specific NSC marker, Nestin, and observed very weak levels of immunoreactivity among migrating cells (data not shown). These results suggest that the vast majority of migrating cells from the lesion site adopt an astrocyte fate and begin migrating after differentiating from the NSC stage to the glial progenitor stage. We also labeled for the mature oligodendrocyte marker, APC (Fig. 5C), and did not detect double-labeling for APC and GFP either rostral or caudal to the lesion/graft site. We also labeled for the myelin marker, myelin basic protein (MBP), and did not detect double-labeling of GFP and MBP (data not shown). Thus, our results demonstrate that glia that adopted an oligodendrocyte fate remained in the lesion/graft site and did not migrate.

3.5. Human graft-derived astrocytes are added to the endogenous population of astrocytes

Based on a previous study of NSC transplantation into the adult mouse spinal cord where human graft-derived astrocytes were found to replace endogenous astrocytes (Chen et al., 2015), we assessed whether human graft-derived astrocytes replaced the endogenous population of astrocytes in the rat spinal cord after injury. Rat astrocytes were defined as GFAP + /DAPI + /hNu- cells while human astrocytes were defined as GFAP + /DAPI + /hNu + cells. The lateral white matter on the grafted side was compared to the lateral white matter on the non-grafted side. C2 spinal cord sections from rats sacrificed 18 months after NSC grafting were used to compare the astrocyte population three segments rostral to the C5 hemisection site, where GFAP + /DAPI + /hNu + human astrocytes were found to migrate most ipsilaterally. No hNu expression was observed among GFAP + /DAPI + /hNu- rat astrocytes on the lateral white matter of the non-grafted side (Fig. 6A). On the grafted side, migrated GFAP + /DAPI + /hNu + human astrocytes were observed among GFAP + /DAPI + /hNu- rat astrocytes in the lateral white matter (Fig. 6B). We quantified the number of human and rat astrocytes in subjects sacrificed 18 months after grafting and found an average of 75.8 ± 6.6 total astrocytes on the non-grafted side and an average of 117.0 ± 9.8 total astrocytes on the grafted side in randomly chosen fields of 800 × 600 pixels at 200× magnification. We detected a statistically significant difference between the total number of astrocytes on the grafted side versus the non-grafted side of the spinal cord at C2 ($t = 3.5$, df = 6, $p = .02$ by Student's t-test) (Fig. 6C). 20% of total astrocytes on the grafted side were GFAP + /DAPI + /hNu + human astrocytes, whereas no astrocytes on the non-grafted side were GFAP + /DAPI + /hNu + (Fig. 6C). No significant difference was detected between the number of GFAP + /DAPI + /hNu- rat

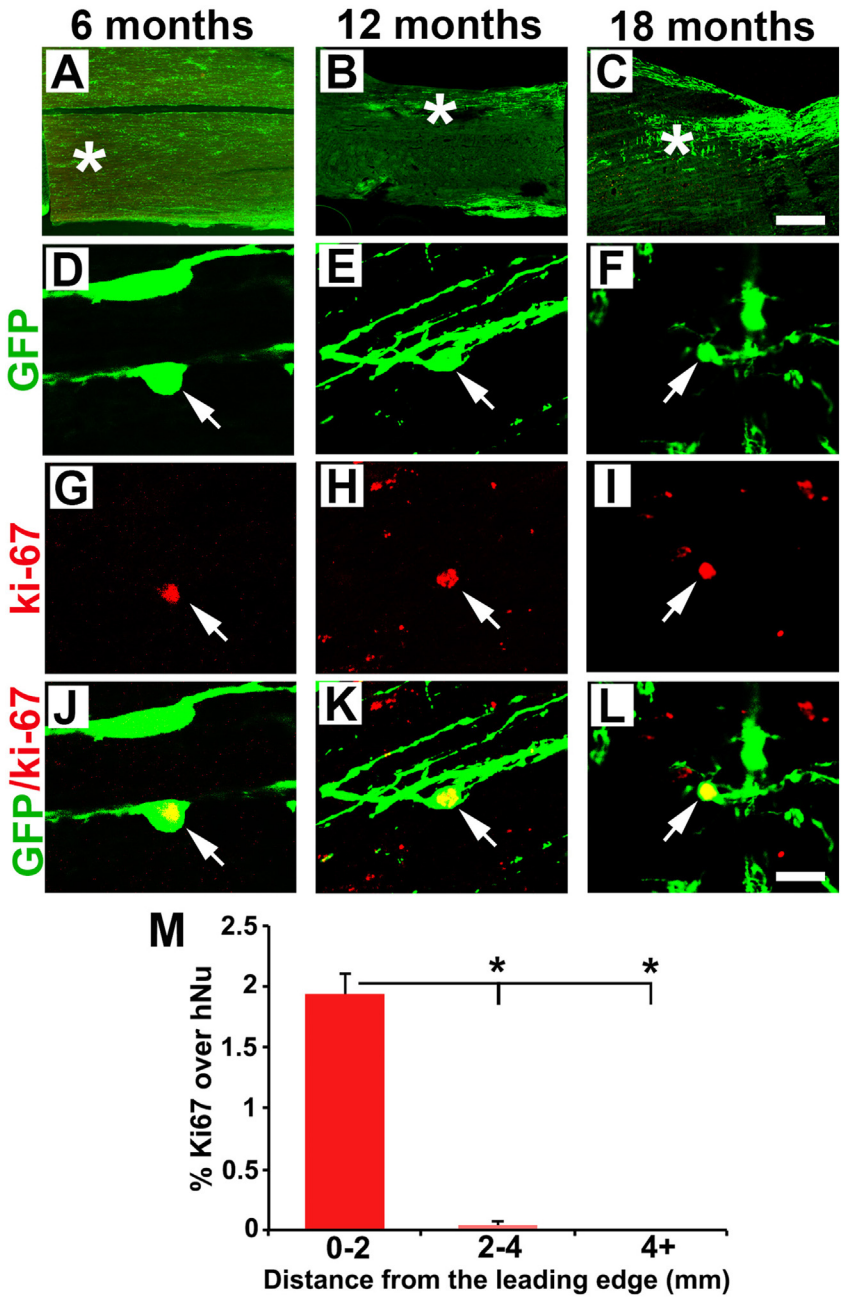

Fig. 4. Human neural stem cells divide at the leading edge of cell migration.
(A–C) Low magnification of **(A)** horizontal spinal cord and **(B–C)** sagittal brainstem sections labeled for GFP and Ki67 showing regions of sampling for panels D–L indicated by *. **(D–L)** Examples of Ki67 + /GFP + nuclei detected at the leading edge of cell migration in subjects sacrificed 6 (D, G, J), 12 (E, H, K), and 18 (F, I, L) months after grafting. **(M)** Quantification of Ki67 + /GFP + nuclei per section at various distances from the leading edge of migration, 18 months after grafting: nearly all dividing cells were located at the leading edge. *P < .05, ANOVA and Wilcoxon test. ± SEM. Scale bar, 500 μm (A-C); 20 μm (D-L).

astrocytes on the non-grafted side versus the grafted side. These data suggest that migrated human graft-derived astrocytes joined the endogenous population of astrocytes in the host rat, increasing the overall population of astrocytes where graft-derived human astrocytes migrated. The increase in the total number of astrocytes in our study involving injured rats differs from reports of graft-derived human astrocytes replacing endogenous mouse astrocytes in intact animals (Han et al., 2013; Chen et al., 2015).

3.6. Human graft-derived astrocytes form a blood-spinal cord barrier

Astrocytes, pericytes, and endothelial cells are known constituents of the BBB and blood-spinal cord barrier (BSCB), with pericytes found between endothelial cells and astrocytic cytoplasmic processes, also known as astrocytic perivascular endfeet (Abbott et al., 2006; Armulik et al., 2010; Bartanusz et al., 2011). Because astrocytes and pericytes regulate the structural integrity of the BBB and BSCB (Armulik et al., 2010), we examined whether human graft-derived astrocytes interact with host pericytes in forming a BSCB at the site of injury. Using the pericyte expression marker, PDGFRβ, and the human specific astrocytic marker, hGFAP, we observed human graft-derived astrocytic endfeet interacting with endogenous pericytes at the lesion/graft site (Fig. 7A-C). To determine whether human astrocytes reform a BSCB at the lesion/graft site, we labeled horizontal spinal cord sections for the endothelial cell marker, RECA1, and human-specific astrocytic marker, hGFAP. We observed human graft-derived astrocytic perivascular endfeet interacting with host endothelial cells at the lesion/graft site (Fig. 7D-G). These data suggest that human graft-derived astrocytes integrated into the host spinal cord and formed a BSCB at the site of injury.

We also labeled coronal C2 sections for RECA1 and hGFAP three spinal cord segments rostral to the lesion/graft site (where migrating astrocytes were present). We observed hGFAP + /GFP + astrocytic perivascular endfeet contacting RECA1 + host endothelium 18 months

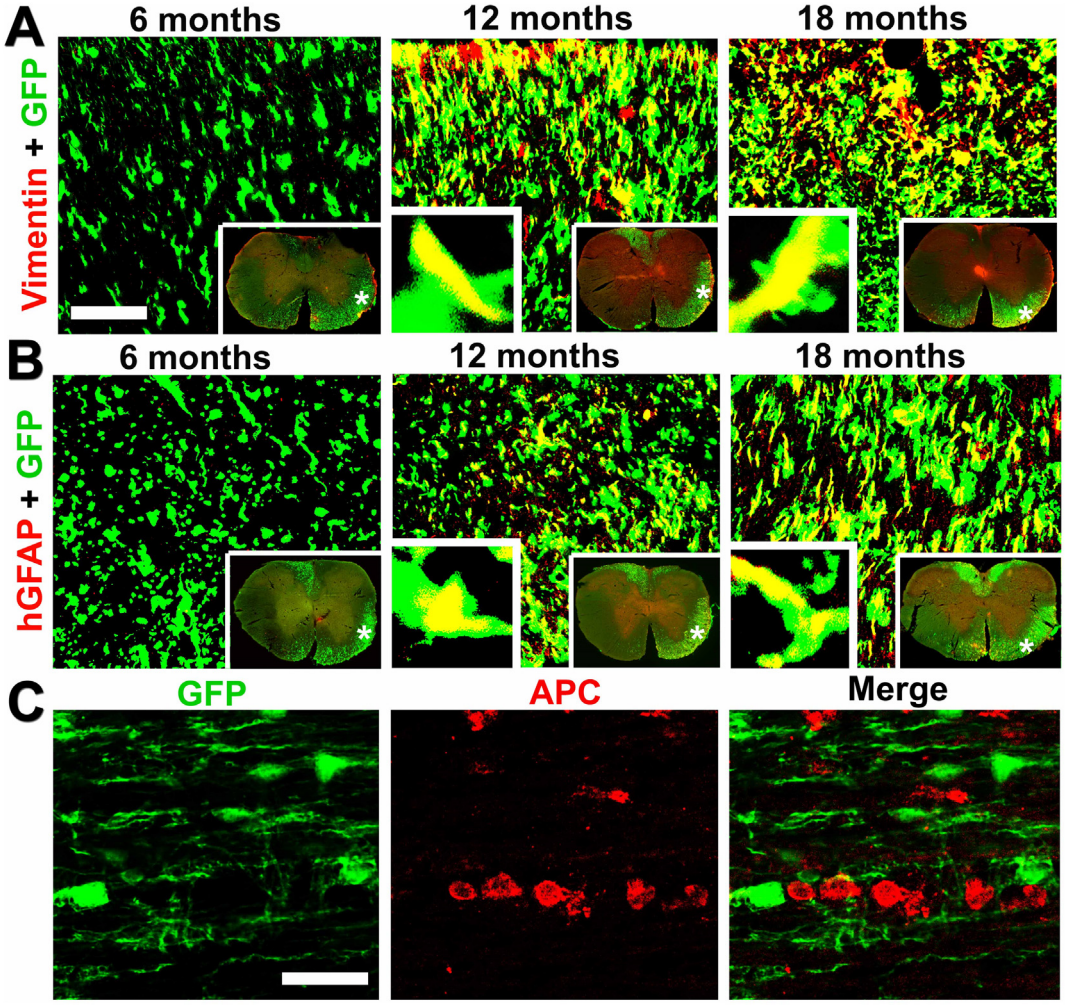

Fig. 5. Migrating human neural stem cells differentiate into glial progenitors and astrocytes but not oligodendrocytes or neurons.
(A–B) Coronal spinal cord sections 6, 12, and 18 months after grafting. Images were taken 3 spinal segments rostral to the lesion/graft site in the ventral white matter. Insets at right low corner show regions of image sampling. Insets at left low corner represent high magnification image of labeled human glial processes. **(A)** At 6 months after grafting, expression of the human-specific glial progenitor marker, vimentin, was not detected among GFP+ axons. By 12 months and 18 months, vimentin was detected in migrating graft-derived human cells. **(B)** At 6 months after grafting, expression of the human-specific astrocytic marker, hGFAP, was not detected among GFP+ axons. By 12 months and 18 months, hGFAP was detected in migrating graft-derived human cells. **(C)** Horizontal spinal cord section at 18 months after grafting at C5. The mature oligodendrocytic marker, APC, did not co-label with migrating GFP+ human graft-derived cells. GFP+ cells also failed to co-localize with neuronal markers (which were entirely absent in these white matter tracts); data not shown. Scale bar, 30 μm (A–B); 10 μm (C).

after grafting (Fig. 7H-I), suggesting that migrated human graft-derived astrocytes also contribute to formation of the BSCB in regions of the CNS unaffected by injury. To determine whether human grafted-derived astrocytes formed perivascular astrocytic networks, we labeled for connexin 43 (CX43), the main gap junction protein expressed in astrocytic perivascular endfeet, which is essential for BBB and BSCB integrity (Chen et al., 2015; Ezan et al., 2012). We detected CX43 expression among the GFP+/GFAP+ perivascular endfeet of migrated human astrocytes (Fig. 7J-L), suggesting the formation of human perivascular astrocytic networks in the rodent and possible involvement in intercellular trafficking of ions and signaling molecules. Notably, the interspecies linkage of human graft-derived astrocytes and endogenous rodent astrocytes has been previously reported (Han et al., 2013). We also found evidence of interspecies connections between the GFP+/GFAP+ perivascular endfeet of human graft-derived astrocytes and the GFAP+ perivascular endfeet of endogenous rat astrocytes coupled by CX43+ gap junctions (Fig. 7J-L).

3.7. Human graft-derived astrocytes widely express glutamate transporter proteins

Astrocytes support neuronal function by regulating neurotransmitter levels and protecting neurons from excitotoxicity (Barres, 2008; Perego et al., 2002). We labeled graft-derived neurons with the somatodendritic marker, MAP2, and found hGFAP+ astrocytic processes closely associated with MAP+ human graft-derived neurons (Fig. 8A). To determine whether human graft-derived astrocytes support neurotransmitter recycling and homeostasis in the lesion site, we labeled for the glutamate transporter, GLT1, which is involved in maintenance of extracellular glutamate concentrations at the synaptic cleft (Perego et al., 2000). We found that GLT1 was expressed widely among human graft-derived astrocytes, with GFAP+/GFP+/GLT1+ processes surrounding GFP+ cells with neuronal morphology (Fig. 8B). These data suggest that graft-derived astrocytes could contribute to synaptic relays formed by graft-derived neurons by maintaining neurotransmitter homeostasis in the lesion/graft site.

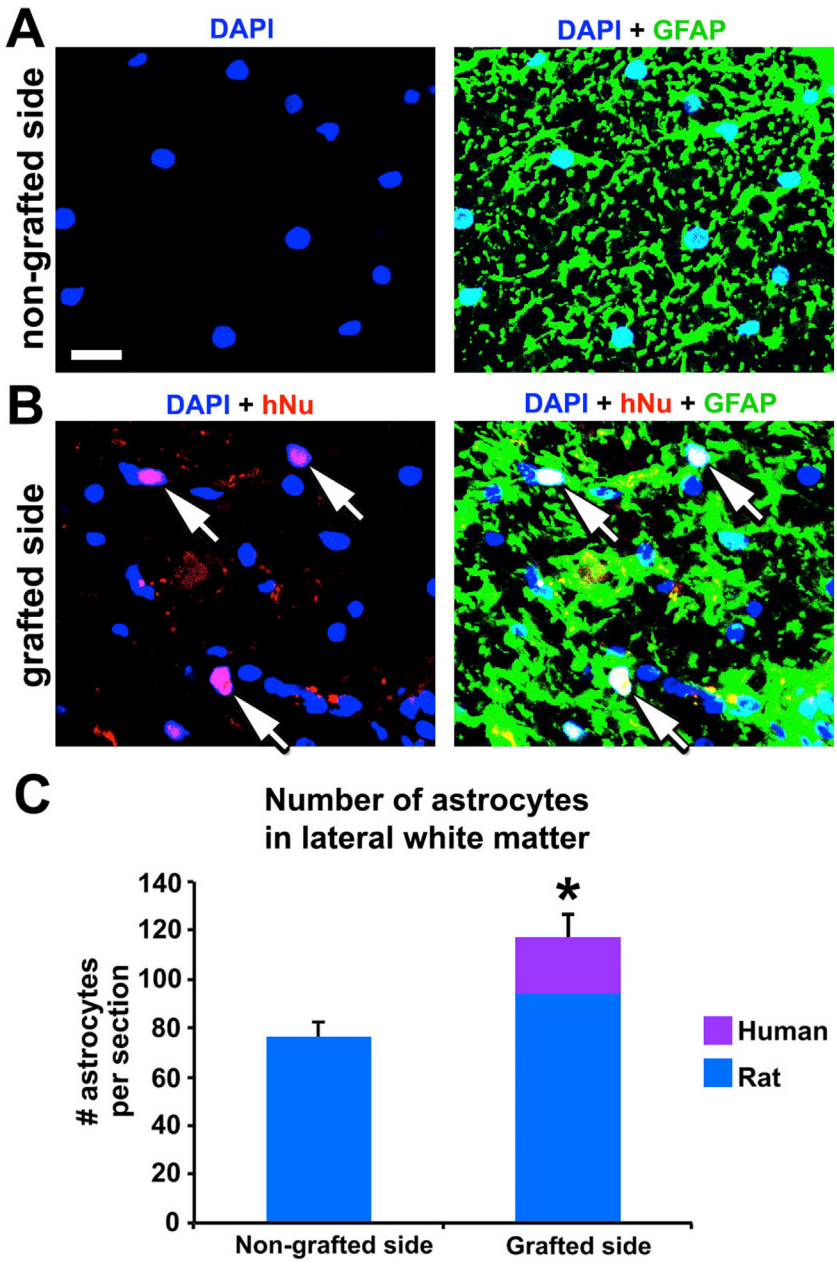

Fig. 6. Migrating graft-derived astrocytes join the endogenous population of astrocytes and increase the overall glial population.
(A) Non-grafted (left) side of spinal cord, white matter: GFAP + /DAPI + /hNu- labeling shows rat astrocytes, three spinal cord segments rostral to the lesion/graft site. Grafts were placed 18 months earlier. hNu immunoreactivity is not observed on the non-grafted side of the spinal cord. **(B)** Grafted (right) side of spinal cord, white matter: Migrating GFAP + /DAPI + /hNu + human astrocytes (arrows) are observed at the same spinal level on the grafted side. Rat astrocytes (GFAP + /DAPI + /hNu-) are also visible. Graft-derived astrocytes were never present in host gray matter (data not shown). **(C)** Quantification of GFAP + /DAPI + /hNu- rat astrocytes and GFAP + /DAPI + /hNu + human astrocytes on non-grafted and grafted sides of the lateral white matter. A significant difference was observed between the total number of astrocytes in the non-grafted side compared to the grafted side. There is no significant difference in the mean number of rat astrocytes on the non-grafted and grafted sides. Mean ± SEM. *P < .05, Student's *t*-test. Scale bar, 15 μm (A–B).

4. Discussion

After transplantation of human NSCs into rat C5 hemisection sites, we observe gradual, long distance migration and differentiation of glial progenitors and astrocytes over a period of 18 months exclusively in host white matter. Thus, the migration of human cells could be interpreted as the continuation of gliogenesis that follows peak neurogenesis, which occurs at an earlier stage after grafting (1–3 months) (Semple et al., 2013; Gallo and Deneen, 2014; Lu et al., 2017). During neural development, migrating glia are repelled from one another via cell-mediated contact inhibition to ensure their even distribution throughout the CNS (Klambt, 2009; Zhan et al., 2017). Thus, a potential mechanism underlying human glial migration from the lesion site could be a limited amount of space in the lesion/graft site that forces proliferating glial progenitors to migrate into host spinal cord and brain.

Grafted NSCs modulate and significantly attenuate reactive astrogliosis surrounding the lesion site, potentially removing a barrier to glial migration. Notably, human glia migrate exclusively in host white matter in the adult CNS environment, suggesting recapitulation of behaviors observed during normal vertebrate gliogenesis where astrocyte progenitors migrate along axonal tracts (Klambt, 2009).

Astrocytes are known to extend perivascular end feet towards blood vessels and take up metabolic substrates such as glucose from the blood, which are trafficked through perivascular astrocytic networks and delivered to neurons in an activity-dependent manner (Rouach et al., 2008; Abbott et al., 2006). Notably, we found that human graft-derived astrocytes appeared to be connected via intraspecies and interspecies CX43 + gap junction channels, possibly forming functional perivascular astrocytic networks involved in intercellular exchange of ions and small molecules. In addition, human graft-derived astrocytes also extended perisynaptic processes expressing GLT1 + glutamate transporter proteins towards human grafted-derived neurons in the lesion/graft site, suggesting a role of graft-derived astrocytes in maintaining extracellular glutamate homeostasis in grafts.

Results of this study have important implications for advancing potential NSC therapies to human clinical trials. The migration of graft-derived astrocytes into uninjured areas of the spinal cord rostral to the SCI site and even into the brainstem could raise safety concerns, but in

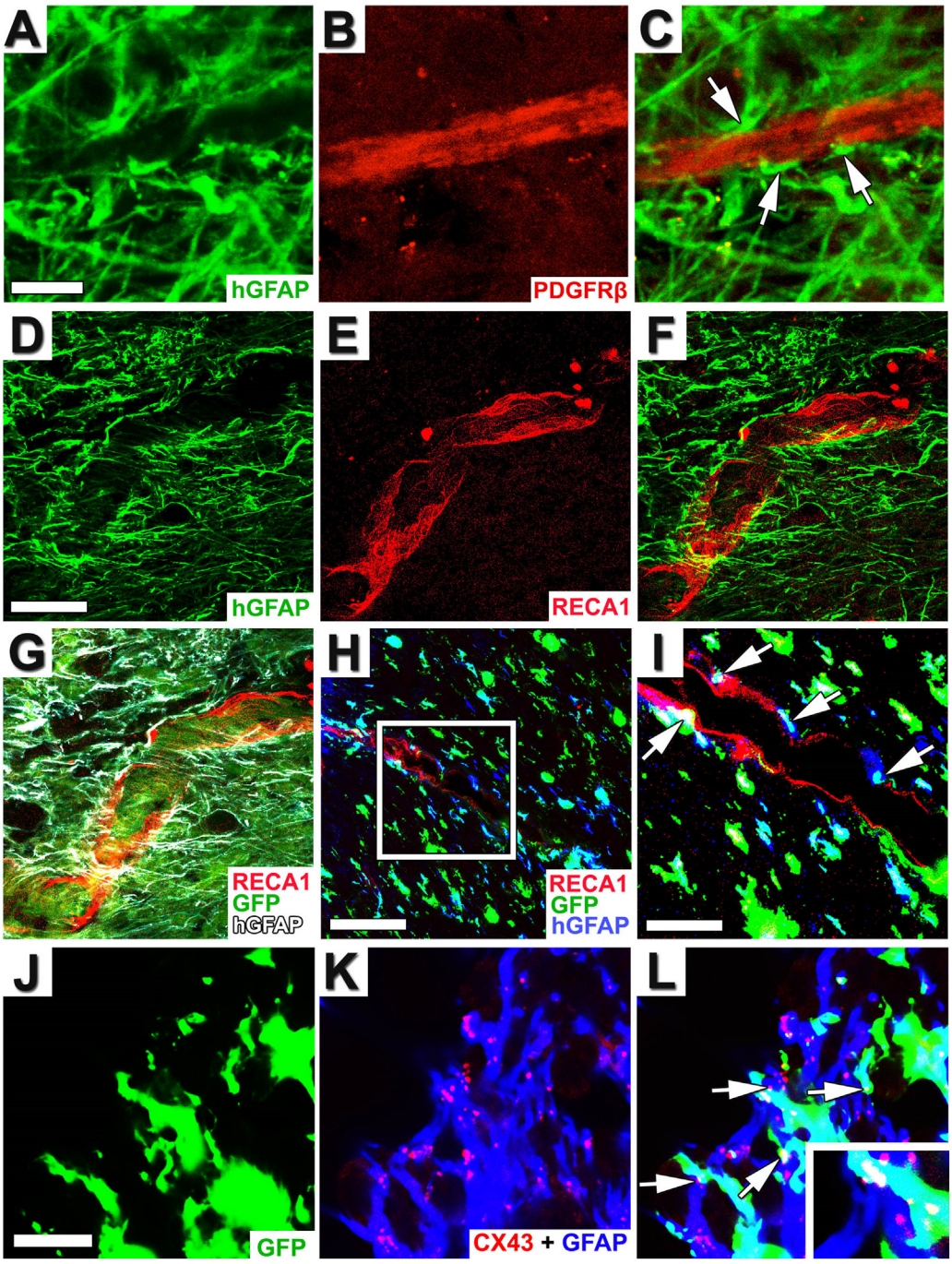

Fig. 7. Graft-derived astrocytes adopt blood-spinal cord barrier phenotypes. **(A-C)** 18 months post-grafting, hGFAP + astrocytic processes are apposed to PDGFRβ+ host pericytes (indicated by arrows) found along vessel-like structures. **(D–F)** hGFAP+ astrocytic processes are closely associated with the surface of a RECA1+ host blood vessel in the graft/lesion site. **(G)** Merged image showing multiple human GFAP+ astrocytic processes (white) closely associated with RECA1+ host endothelium (red) in the lesion/graft site among other GFP + grafted cells (green). **(H–I)** Gliovascular units (in cyan) form between hGFAP+/GFP+ processes and RECA1+ host endothelium, 3 spinal cord segments rostral to the lesion/graft site in host white matter. Arrows indicate close association of GFP +/hGFAP+ processes from migrated astrocytes with a RECA+ host blood vessel. **(J-K)** Labeling for **GFP** (graft cells), **GFAP** (detects both graft- and host-derived astrocytes), and the astrocytic gap junction protein, **CX43**. Merged image in **(L)** suggests that graft and host astrocytic processes are connected by CX43+ gap junctions (regions of white co-labeling, indicated by arrows). Inset shows higher magnification image of GFAP+ processes and GFP+/GFAP+ processes expressing CX43 (J-L). All images were taken 18 months after grafting. Scale bar, 8 μm (A–C); 50 μm (D-H); 17 μm (I); 20 μm (J–L). (For interpretation of the references to colour in this figure legend, the reader is referred to the web version of this article.)

the present study, this migration was not associated with detectable adverse consequences. Indeed, we reported earlier (Lu et al., 2017) that these grafts result in significant improvements in skilled forelimb motor function without detectable adverse functional outcomes. Moreover, human graft-derived astrocytes that migrated rostral to the lesion site surrounded host endothelial cells and pericytes in uninjured areas of the spinal cord, and formed astrocytic networks coupled by gap junction channels, suggesting integration in the host BSCB. Moreover, Zhang and colleagues have reported that locomotor function in mice is unaffected by migration and integration of human neural progenitor-derived astrocytes when transplanted into intact spinal cords (Chen et al., 2015). Thus, at present, there is no evidence that migration and integration of graft-derived glia have deleterious outcomes, and results of the present study contribute to the safety profile of these cells.

Several preclinical studies have demonstrated the safety and efficacy of NSC transplantation for partially restoring motor function in rodent and now primate models of SCI (Lu et al., 2012; Lu et al., 2014; Kadoya et al., 2016; Lu et al., 2017; Rosenzweig et al., 2018), highlighting the therapeutic potential of this cell replacement model. Our results show that transplanted H9 human NSCs in sites of SCI can attenuate reactive astrogliosis and differentiate into astrocytes that survive, migrate, and functionally integrate into the host rodent CNS over a period of 1.5 years. In addition, these human NSCs support host rodent axon regeneration and formation of functional synaptic relays across the SCI site that support late recovery of motor function (Lu et al., 2017). Human NSC transplantation into spinal cord lesion sites remains a candidate translational therapy for SCI.

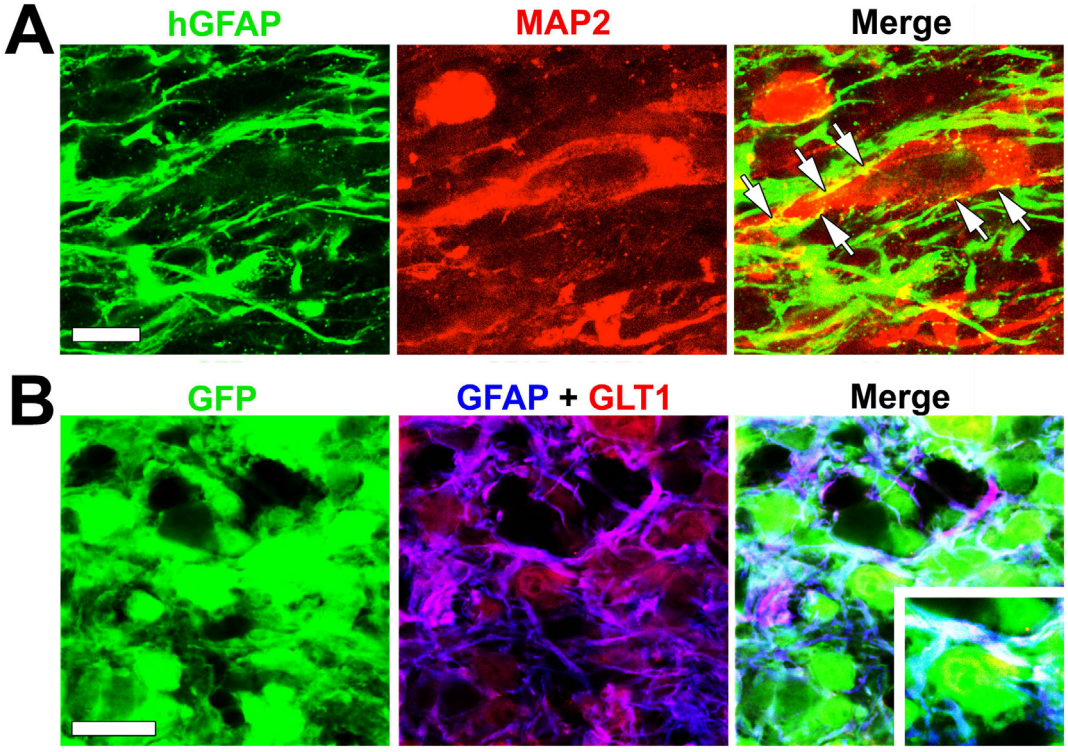

Fig. 8. Graft-derived astrocytes surround neurons and express glutamate transporter proteins within stem cell grafts.
(A) hGFAP+ astrocytic processes associated with MAP2+ graft-derived neuron at the somatodendritic domain (yellow regions in Merge panel, indicated by arrows. Images were taken from center of an 12-month graft). **(B)** High magnification view demonstrates that astrocytic processes within grafts (GFAP+) are co-localized with the glutamate transporter (**GLT1**). All cells in this region are GFP-labeled, indicating that human NSC-derived graft astrocytes express glutamate transporters (white regions in Merged panel). Inset shows higher magnification. All images are from 12-month grafts. Scale bar, 10 μm (A); 20 μm (B) (For interpretation of the references to colour in this figure legend, the reader is referred to the web version of this article.)

Acknowledgements

This work was supported by the Veterans Administration (Gordon Mansfield Collaborative Consortium [1I50RX001706-01]) and Merit Review Grants [1 I01 BX001252-01A2 and 1 I21 RX00084-01A1]), NIH (NS09881 and EB014986), the Craig H. Neilsen Foundation, the California Institute for Regenerative Medicine, the Dr. Miriam and Sheldon G. Adelson Medical Research Foundation and the Bernard and Anne Spitzer Charitable Trust.

References

Abbott, N.J., Ronnback, L., Hansson, E., 2006. Astrocyte–endothelial interactions at the blood–brain barrier. Nat. Rev. Neurosci. 7, 41–53.
Anderson, M.A., Burda, J.E., Ren, Y., Ao, Y., O'Shea, T.M., Kawaguchi, R., Coppola, G., Khakh, B.S., Deming, T.J., Sofroniew, M.V., 2016. Astrocyte scar formation aids central nervous system axon regeneration. Nature 532, 195–200.
Armulik, A., Genove, G., Mae, M., Nisancioglu, M.H., Wallgard, E., Niaudet, C., He, L., Norlin, J., Lindblom, P., Strittmatter, K., Johansson, B.R., Betsholtz, C., 2010. Pericytes regulate the blood–brain barrier. Nature 468, 557–561.
Barres, B.A., 2008. The mystery and magic of glia: a perspective on their roles in health and disease. Neuron 60, 430–440.
Bartanusz, V., Jezova, D., Alajajian, B., Digicaylioglu, M., 2011. The blood–spinal cord barrier: morphology and clinical implications. Ann. Neurol. 70, 194–206.
Brustle, O., Choudhary, K., Karram, K., Huttner, A., Murray, K., Dubois-Dalcq, M., McKay, R.D.G., 1998. Chimeric brains generated by intraventricular transplantation of fetal human brain cells into embryonic rats. Nat. Biotechnol. 16, 1040–1044.
Canoll, P., Goldman, J.E., 2008. The interface between glial progenitors and gliomas. Acta Neuropathol. 116, 465–477.
Chen, H., Qian, K., Chen, W., Hu, B., Blackbourn, L.W., Du, Z., Ma, L., Liu, H., Knobel, K.M., Ayala, M., Zhang, S.C., 2015. Human-derived neural progenitors functionally replace astrocytes in adult mice. J. Clin. Invest. 125, 1033–1042.
Ezan, P., Andre, P., Cisternino, S., Saubamea, B., Boulay, A.-C., Doutremer, S., Thomas, M.-A., Quenech'du, N., Giaume, C., Cohen-Salmon, M., 2012. Deletion of astroglial connexins weakens the blood–brain barrier. J. Cereb. Blood Flow Metab. 32, 1457–1467.
Fawcett, J.W., 2009. Recovery from spinal cord injury: regeneration, plasticity and rehabilitation. Brain 132, 1417–1418.
Gallo, V., Deneen, B., 2014. Glial development: the crossroads of regeneration and repair in the CNS. Neuron 83, 283–308.
Haas, C., Fischer, I., 2013. Human astrocytes derived from glial restricted progenitors support regeneration of the injured spinal cord. J. Neurotrauma 30, 1035–1052.
Han, X., Chen, M., Wang, F., Windrem, M., Wang, S., Shanz, S., Xu, Q., Oberheim, N.A., Bekar, L., Betstadt, S., Silva, A.J., Takano, T., Goldman, S.A., Nedergaard, M., 2013. Forebrain engraftment by human glial progenitor cells enhances synaptic plasticity and learning in adult mice. Cell Stem Cell 12, 342–353.
Han, S.S.W., Liu, Y., Tyler-Polsz, C., Rao, M.S., Fischer, I., 2004. Transplantation of glial-restricted precursor cells into the adult spinal cord: survival, glial-specific differentiation, and preferential migration in white matter. Glia 45, 1–16.
Hawryluk, G.W.J., Spano, S., Chew, D., Wang, S., Erwin, M., Chamankhah, M., Forgione, N., Fehlings, M.G., 2014. An examination of the mechanisms by which neural precursors augment recovery following spinal cord injury: a key role for remyelination. Cell Transplant. 23, 365–380.
Jin, Y., Neuhuber, B., Singh, A., Bouyer, J., Lepore, A., Bonner, J., Himes, T., Campanelli, J.T., Fischer, I., 2011. Transplantation of human glial restricted progenitors and derived astrocytes into a contusion model of spinal cord injury. J. Neurotrauma 28, 579–594.
Jones, L.L., Tuszynski, M.H., 2002. Spinal cord injury elicits expression of keratan sulfate proteoglycans by macrophages, reactive microglia, and oligodendrocyte progenitors. J. Neurosci. 22, 4611–4624.
Kadoya, K., Lu, P., Nguyen, K., Lee-Kubli, C., Kumamaru, H., Yao, L., Knackert, J., Poplawski, G., Dulin, J.N., Strobl, H., Takashima, Y., Biane, J., Conner, J., Zhang, S.C., Tuszynski, M.H., 2016. Spinal cord reconstitution with homologous neural grafts enables robust corticospinal regeneration. Nat. Med. 22, 479–487.
Karimi-Abdolrezaee, S., Eftekharpour, E., Wang, J., Morshead, C.M., Fehlings, M.G., 2006. Delayed transplantation of adult neural precursor cells promotes remyelination and functional neurological recovery after spinal cord injury. J. Neurosci. 26, 3377–3389.
Keirstead, H.S., Nistor, G., Bernal, G., Totoiu, M., Cloutier, F., Sharp, K., et al., 2005. Human embryonic stem cell-derived oligodendrocyte progenitor cell transplants remyelinate and restore locomotion after spinal cord injury. J. Neurosci. 25, 4694–4705.
Klambt, C., 2009. Modes and regulation of glial migration in vertebrates and invertebrates. Nat. Rev. Neurosci. 10, 769.
Lepore, A.C., Han, S.S.W., Tyler-Polsz, C.J., Cai, J., Rao, M.S., Fischer, I., 2004. Differential fate of multipotent and lineage-restricted neural precursors following transplantation into the adult CNS. Neuron Glia Biol. 1, 113–126.
Lu, P., Ceto, S., Wang, Y., Graham, L., Wu, D., Kumamaru, H., Staufenberg, E., Tuszynski,

M.H., 2017. Prolonged human neural stem cell maturation supports recovery in injured rodent CNS. J. Clin. Investig. 127, 3287–3299.
Lu, P., Wang, Y., Graham, L., McHale, K., Gao, M., Wu, D., Brock, J., Blesch, A., Rosenzweig, E.S., Havton, L.A., Zheng, B., Conner, J.M., Marsala, M., Tuszynski, M.H., 2012. Long-distance growth and connectivity of neural stem cells after severe spinal cord injury. Cell 150, 1264–1273.
Lu, P., Woodruff, G., Wang, Y., Graham, L., Hunt, M., Wu, D., Boehle, E., Ahmad, R., Poplawski, G., Brock, J., Goldstein, L.S., Tuszynski, M.H., 2014. Long-distance axonal growth from human induced pluripotent stem cells after spinal cord injury. Neuron 83, 789–796.
Perego, C., Vanoni, C., Bossi, M., Massari, S., Basudev, H., Longhi, R., Pietrini, G., 2000. The GLT-1 and GLAST glutamate transporters are expressed on morphologically distinct astrocytes and regulated by neuronal activity in primary hippocampal co-cultures. J. Neurochem. 75, 1076–1084.
Rosenzweig, E.S., Brock, J.H., Lu, P., Kumamaru, H., Salegio, E.A., Kadoya, K., Weber, J.L., Liang, J.J., Moseanko, R., Hawbecker, S., Huie, J.R., Havton, L.A., Nout-Lomas, Y.S., Ferguson, A.R., Beattie, M.S., Bresnahan, J.C., Tuszynski, M.H., 2018. Restorative effects of human neural stem cell grafts on the primate spinal cord. Nat. Med. 24, 484.
Rouach, N., Koulakoff, A., Abudara, V., Willecke, K., Giaume, C., 2008. Astroglial Metabolic Networks Sustain Hippocampal Synaptic Transmission. Science 322, 1551–1555.
Salewski, R.P., Mitchell, R.A., Li, L., Shen, C., Milekovskaia, M., Nagy, A., Fehlings, M.G., 2015. Transplantation of induced pluripotent stem cell-derived neural stem cells mediate functional recovery following thoracic spinal cord injury through remyelination of axons. Stem Cells Transl. Med. 4, 743–754.
Schitine, C., Nogaroli, L., Costa, M.R., Hedin-Pereira, C., 2015. Astrocyte heterogeneity in the brain: from development to disease. Front. Cell. Neurosci. 9, 1–11.
Semple, B.D., Blomgren, K., Gimlin, K., Ferriero, D.M., Noble-Haeusslein, L.J., 2013. Brain development in rodents and humans: Identifying benchmarks of maturation and vulnerability to injury across species. Prog. Neurobiol. 106 (107), 1–16.
Silver, J., Miller, J.H., 2004. Regeneration beyond the glial scar. Nat. Rev. Neurosci. 5, 146–156.
Smith, G.M., Miller, R.H., Silver, J., 1986. Changing role of forebrain astrocytes during development, regenerative failure, and induced regeneration upon transplantation. J. Comp. Neurol. 251, 23–43.
Sofroniew, M.V., Vinters, H.V., 2010. Astrocytes: biology and pathology. Acta Neuropathol. 119, 7–35.
Thomson, J.A., Itskovitz-Eldor, J., Shapiro, S.S., Waknitz, M.A., Swiergiel, J.J., Marshall, V.S., Jones, J.M., 1998. Embryonic stem cell lines derived from human blastocysts. Science 282, 1145–1147.
Tien, A.-C., Tsai, H.-H., Molofsky, A.V., McMahon, M., Foo, L.C., Kaul, A., Dougherty, J.D., Heintz, N., Gutmann, D.H., Barres, B.A., Rowitch, D.H., 2012. Regulated temporal-spatial astrocyte precursor cell proliferation involves BRAF signalling in mammalian spinal cord. Development 139, 2477–2487.
Windrem, M.S., Schanz, S.J., Morrow, C., Munir, J., Chandler-Militello, D., Wang, S., Goldman, S.A., 2014. A competitive advantage by neonatally engrafted human glial progenitors yields mice whose brains are chimeric for human glia. J. Neurosci. 34, 16153–16161.
Zhan, J.S., Gao, K., Chai, R.C., Jia, X.H., Luo, D.P., Ge, G., Jiang, Y.W., Fung, Y.W., Li, L., Yu, A.C.H., 2017. Astrocytes in migration. Neurochem. Res. 42, 272–282.
Zhang, S.-C., Wernig, M., Duncan, I.D., Brustle, O., Thomson, J.A., 2001. In vitro differentiation of transplantable neural precursors from human embryonic stem cells. Nat. Biotechnol. 19, 1129–1133.